Non-equilibrium coexistence between a fluid and a hotter or colder crystal of granular hard disks

R. Maire, A. Plati, F. Smallenburg, G. Foffi

Non-equilibrium coexistence between a fluid and a hotter or colder crystal of granular hard disks

R. Maire,[1] A. Plati,[1] F. Smallenburg,[1] and G. Foffi[1,*]

[1] *Université Paris-Saclay, CNRS, Laboratoire de Physique des Solides, 91405 Orsay, France*

(Dated: November 24, 2025)

Non-equilibrium phase coexistence is commonly observed in both biological and artificial systems, yet understanding it remains a significant challenge. Unlike equilibrium systems, where free energy provides a unifying framework, the absence of such a quantity in non-equilibrium settings complicates their theoretical understanding. Granular materials, driven out of equilibrium by energy dissipation during collisions, serve as an ideal platform to investigate these systems, offering insights into the parallels and distinctions between equilibrium and non-equilibrium phase behavior. For example, the coexisting dense phase is typically colder than the dilute phase, a result usually attributed to greater dissipation in denser regions. In this article, we demonstrate that this is not always the case. Using a simple numerical granular model, we show that a hot solid and a cold liquid can coexist in granular systems. This counterintuitive phenomenon arises because the collision frequency can be lower in the solid phase than in the liquid phase, consistent with equilibrium results for hard-disk systems. We further demonstrate that kinetic theory can be extended to accurately predict phase temperatures even at very high packing fractions, including within the solid phase. Our results highlight the importance of collisional dynamics and energy exchange in determining phase behavior in granular materials, offering new insights into non-equilibrium phase coexistence and the complex physics underlying granular systems.

I. INTRODUCTION

The theory of equilibrium phase coexistence as formalized by Gibbs establishes that mechanical, thermal, and chemical equilibrium are necessary conditions for the stability of a heterogeneous substance at equilibrium [1]. With the recent advancements in non-equilibrium statistical physics, it has become evident that phase coexistence phenomena are equally ubiquitous in out-of-equilibrium systems [2–4] and that Gibbs' equilibrium conditions must be relaxed for example in active matter systems or in driven chemical phase transitions [4, 5]. This realization has sparked significant theoretical and experimental efforts to explore the differences and similarities between these non-equilibrium cases and their well-known equilibrium counterparts [6–13]. Several peculiarities characterize phase coexistence in non-equilibrium systems. For instance, in active systems, the common tangent construction fails and must be replaced by alternative constructions based on an effective free energy [14]. Likewise, the bulk density of the coexisting phases may depend on the effective surface tension [15, 16], highlighting the system's deviation from a conventional underlying free energy. Out of equilibrium, the coarsening dynamics are also unusual, with phenomena such as non-standard roughness of interfaces at coexistence [17, 18], peculiar growth of length scales during coarsening [5, 19, 20] and reversed Ostwald ripening leading to bubbly phases [21, 22] or microphase separation [23]. While surface tension between phases can still be defined following different equilibrium definitions, these approaches can yield different results in non-equilibrium systems [24–27]. Similarly, macroscopic heat flux between phases and peculiar interfacial properties can be observed in boundary-driven systems [28–32]. Dynamic phenomena such as traveling [33, 34], pattern-forming [35, 36], and even chasing coexisting phases [37] have been observed as well.

Recently, inspired by biological active systems, a growing interest in underdamped self-propelled particles surfaced [38–41]. Among other things, it has been observed that these particles can undergo a motility-induced phase separation [42–44], with a dense phase colder [45] than the dilute one due to reduced effective self-propulsion in the dense phase [5]. This highly non-equilibrium effect was recently observed in an experimental system [46]. In contrast, Ref. 47 reported motility-induced phase separation resulting in a hotter solid. Similar observations, in stark contrast to Gibbs' requirement of thermal equilibrium, were previously made in the study of vibrated granular media, where gas-liquid [48–59] and liquid-solid phase coexistence [60–70] consistently revealed a colder dense phase. These results have traditionally been explained by the assumption that the denser phase must dissipate more energy, and therefore be colder, due to a higher collision frequency compared to the coexisting dilute phase.

Nonetheless, a hotter solid was recently observed in a driven 2D granular system [71]. This phenomenon was however attributed to boundary effects rather than induced by the inter-particle interaction. In a recent realistic numerical study of a vibrated quasi-2D granular system, we also surprisingly observed that a crystal composed of bidisperse beads can exhibit a hotter solid than the coexisting liquid [72]. This temperature difference partially arose from geometric effects that cannot occur in a monodisperse system. In this paper, we simplify the

* giuseppe.foffi@universite-paris-saclay.fr

previously used model by employing only monodisperse beads and demonstrate that even for such simple systems, it is possible to find a solid phase hotter than the coexisting liquid. Surprisingly, we find that dissipation during collisions can be the key mechanism for a hotter solid. By developing a kinetic theory to explain these results, we show that, although the solid phase is always denser, its particle collision frequency is typically lower than in the coexisting liquid, reducing dissipation and enabling the solid to be hotter.

The paper is organized as follows: in Sec. II, we present and simulate a simple 2D granular model in the liquid-solid coexistence region, showing how a hotter solid can emerge. In Sec. III, we explain this behavior using an equilibrium-like argument based on the collision frequency of hard-disk coexisting phases, and then extend the discussion with a fully non-equilibrium theory. Finally, in Sec. IV, we discuss the relevance and broader implications of our findings.

II. NUMERICAL INVESTIGATIONS

To explore the temperature differences between the coexisting liquid and solid phases in a system of dissipative hard disks, we consider a simple model system in two distinct limits. In this section, we describe both the model and the simulation methods we use to study them.

A. The model

A quasi-2D vibrated box serves as a paradigmatic system for investigating driven granular systems [67, 73–82]. In this setup, particles are confined within a quasi-2D horizontal plane, bounded by parallel top and bottom plates. The system is driven by vertical vibrations of the container, which inject energy into the vertical degrees of freedom of the particles. This energy is subsequently dissipated and redistributed across the horizontal plane through inter-particle collisions.

To capture the essential physics of the quasi-2D system, we propose the following 2D coarse-grained model. The system is made of 2D dissipative hard disks of mass m and diameter σ. When two particles collide, they can both dissipate energy and gain momentum, leading to the following collision rule [73, 83]:

$$\begin{aligned} \boldsymbol{v}_i' &= \boldsymbol{v}_i - \left[\frac{1+\alpha}{2}(\boldsymbol{v}_{ij}\cdot\hat{\boldsymbol{\sigma}}_{ij}) + \Delta\right]\hat{\boldsymbol{\sigma}}_{ij} \\ \boldsymbol{v}_j' &= \boldsymbol{v}_j + \left[\frac{1+\alpha}{2}(\boldsymbol{v}_{ij}\cdot\hat{\boldsymbol{\sigma}}_{ij}) + \Delta\right]\hat{\boldsymbol{\sigma}}_{ij}, \end{aligned} \tag{1}$$

where $\boldsymbol{v}_i'$ is the post-collisional velocity of particle i, while $\hat{\boldsymbol{\sigma}}_{ij}$ and $\boldsymbol{v}_{ij}$ are respectively the unit vector joining particles i and j and the relative velocity between them. The coefficient of restitution $0 < \alpha < 1$ governs the dissipation during collisions, and $\Delta > 0$ is responsible for velocity injection. This velocity injection mimics the energy redistribution during grain-grain collisions in the quasi-2D system described above. The energy change during a collision can be either positive or negative, depending on the relative velocity of the particles. For large relative velocities, $|\boldsymbol{v}_{ij}| \gg \Delta$ and sufficiently small α, the term proportional to α dominates, leading to dissipative collisions. Conversely, at low relative velocities, energy dissipation through α is minimal, and instead, particles gain an additional velocity Δ, effectively injecting energy into the system.

Between collisions, the hard disks are also coupled to an external bath at granular temperature T_b with drag γ via a Langevin equation:

$$\frac{\mathrm{d}\boldsymbol{v}}{\mathrm{d}t} = -\gamma\boldsymbol{v} + \sqrt{2\gamma T_b/m}\boldsymbol{\eta}, \tag{2}$$

where $\boldsymbol{\eta}$ is a random vectorial white Gaussian noise with unit variance and zero mean. Comparing again to a vibrated quasi-2D granular system, this effective noise would represent the roughness of the top and bottom plates confining the particles in the realistic quasi-2D model. Collisions with these plates cause the hard disks to behave as Brownian particles on the horizontal plane for time scales larger than the one set by the frequency of the shaking [84, 85].

We focus on two limiting cases of interest:

- The $\Delta + \gamma$ *model*, where $T_b = 0$ [73, 86]. Here, particles lose energy during their free flight according to $v(t) = v_0 e^{-\gamma t}$ while collisions, on average, increase the system's energy—though in some cases, they may also lead to energy loss. This 2D model is representative of a quasi-2D system in a dynamical regime where particles are shaken with sufficient energy to undergo strong collisions with both the lower and the upper plate. γ effectively accounts for the horizontal energy loss due to tangential friction with the smooth plates, while Δ reproduces the energy transfer between the vertical and horizontal degrees of freedom at collision. The equilibrium limit corresponds to $\Delta \to 0$, $\alpha \to 1$ and $\gamma \to 0$.

- The *granular Langevin model* (GLM), where $\Delta = 0$ [72, 84]. In this case, all the energy is supplied by the bath, and collisions only dissipate energy. In the quasi-2D system, this corresponds to grains confined between rough plate that are not strongly shaken, which limits their vertical motion and interaction with the upper plate. In this regime, surface asperities transfers energy primarily into the horizontal plane during grain-plate collisions, while grain-grain collisions contribute minimally to the energy change in the horizontal plane. In the limit $\alpha \to 1$ we recover an equilibrium system.

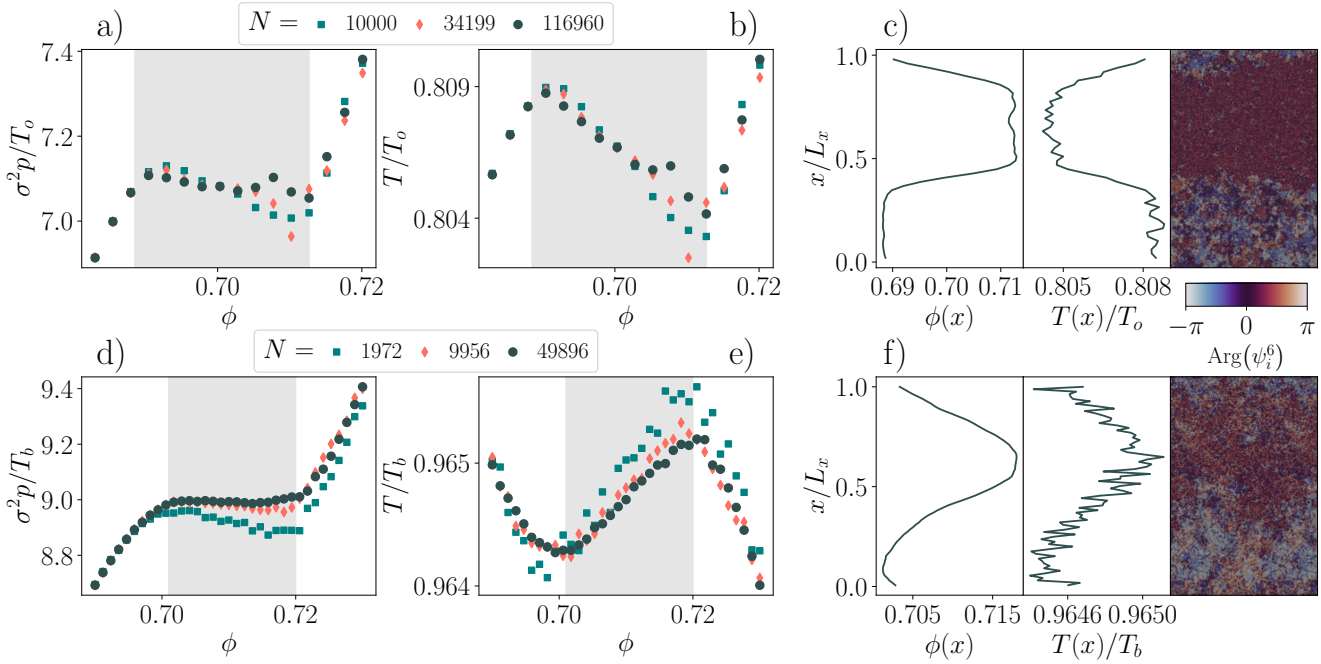

FIG. 1. Top: $\Delta+\gamma$ model ($\Delta/\sigma\gamma = 1.1$ and $\alpha = 0.95$), bottom: GLM ($T_b/m(\sigma\gamma)^2 = 0.125$ and $\alpha = 0.99$). a) and d): Pressure as a function of the density. b) and e): Energy as a function of the density. First two panels of c) and f): Granular temperature and density averaged over a y slab in $[x, x+10\sigma]$. Last panel of c) and f): Snapshot of a liquid-solid coexistence, particles are colored by the angle of hexatic local order parameter $\mathrm{Arg}(\psi_i^6)$ with $\psi_i^6 = \sum_{j=1}^{N_i} e^{i6\theta_{ij}}/N_i$, with N_i the number of neighbors to particle i and θ_{ij} the angle in real space between i and j. The density and temperature profiles in c) represent time-averaged values over 2×10^4 measurements of the properties obtained from the time evolution of the displayed snapshot. The measurement window is sufficiently small to ensure that large variations in the density field remain negligible. The coexistence behavior of the GLM is more challenging to visualize compared to that of the $\Delta+\gamma$ model. This difficulty arises because its behavior closely mirrors the equilibrium liquid-hexatic phase coexistence, where the transition between the two phases is extremely weak, resulting in strongly fluctuating interfaces [87]. For this system, the profiles are obtained by averaging 10^5 snapshots over 60 independent realizations. Before performing the averaging, all particles are shifted such that the center of mass [88] is positioned at $x/L_x = 0.75$ ensuring that the solid phase consistently resides in the region $0.5 < x/L_x < 1$ [89, 90]. Therefore, unlike in the $\Delta+\gamma$ model, the snapshot of the GLM in f) does not correspond to the ones used to extract the profiles. Note finally that for the $\Delta+\gamma$ model, the lack of a thermal bath means there is no obvious external reference temperature to compare the measured T to. Hence, for this system, we plot the temperature in terms of T_o, which we define as the theoretical temperature of the Delta model assuming velocity distributed as a Gaussian and in the absence of drag ($\gamma = 0$). It is given by [83] $T_o = \frac{1}{2}m\Delta^2\left(\alpha\sqrt{\pi}/2 + \sqrt{\alpha^2\pi/4 + (1-\alpha)^2}\right)^2/(1-\alpha^2)^2$ and is independent on the density.

B. Numerical simulations

Using event-driven molecular dynamics [91] we simulate both models described above using up to $N \simeq 10^5$ particles in boxes of size $L_x \times L_y$ with periodic boundary conditions. We define $\phi = N\pi(\sigma/2)^2/L_xL_y$ as the packing fraction of the system and focus on the region near the equilibrium liquid-hexatic transition. For simplicity, we will refer to the crystalline or hexatic phase in coexistence with the liquid as the "solid phase" of the system without making a distinction between the two.

The granular temperature T of the system is defined as [92, 93]:

$$T = \frac{1}{2}m\sum_{i=1}^{N}\langle \boldsymbol{v}_i^2\rangle, \tag{3}$$

where $\langle\dots\rangle$ represents a time average. When explicitly stated, it also includes an average over different initial conditions. Additionally, we define the pressure p as the virial pressure (see Appendix. A):

$$p = \frac{NT}{L_xL_y} + \frac{m\sigma}{2L_xL_yt}\sum_{\text{coll-ij}}\left(\frac{1+\alpha}{2}\left(\boldsymbol{v}_{ij}\cdot\hat{\boldsymbol{\sigma}}_{ij}\right)+\Delta\right). \tag{4}$$

We present the results of our simulations in the coexistence region of the liquid-solid phase transition in Fig. 1. The top panels show the results for the $\Delta+\gamma$ model, while the bottom panels display the results for the GLM. For the $\Delta+\gamma$ model, we observe a Mayer-Wood loop [87, 94, 95] in the pressure (Panel a), indicating a first-order phase transition. More intriguingly, in the coexistence region, the granular temperature also exhibits a

non-monotonic trend (Panel b). Unlike the loop in pressure, this phenomenon is not related to interfacial effects, as it does not disappear with increasing N. Instead, it is most likely associated with the coexistence of two phases at different temperatures. Indeed, if the existence of a lever-rule for the density field is assumed [72], the temperature field which is slaved to the density and crystallization field should also follow a lever-rule. As the density increases, a larger fraction of the system transitions to the solid phase, following the conventional lever-rule for the density field. Consequently, a greater portion of the system attains the temperature of the solid. Since in Panel b the global temperature decreases, we hypothesize that the coexisting solid phase is colder than the coexisting liquid phase. This is confirmed by direct computations of the temperature $T(x)$ and density $\phi(x)$ profiles, corresponding to a given phase separation, averaged over multiple realizations and snapshots (Panels c). For the GLM, the pressure loop is still evident (Panel d), indicating a first-order phase transition. The temperature also presents the expected non-monotonic trend (Panel e), but in this case, the solid is hotter than the liquid, as the global temperature increases. This observation is corroborated by direct computations of the local temperature and densities (Panels f).

Therefore, we find a solid that is hotter than the liquid in the GLM, even though the collisions are purely dissipative. Surprisingly, in the $\Delta + \gamma$ model, where energy is injected during collisions, the solid is colder.

Before delving into the theory explaining these intriguing results, we note that, both for the GLM and the $\Delta + \gamma$ model, the energy difference between the two phases is rather low (i.e. between 0.1 and 0.3 %). This rather small temperature difference ultimately stems from the small density difference between the liquid and the solid, as well as our choice of parameters, which keeps the system relatively close to equilibrium. Maintaining this proximity to equilibrium is essential for the validity of the theoretical framework we will develop. Additionally, we point out that in the GLM, further increasing dissipation readily leads to a continuous phase transition and the disappearance of the phase coexistence. This phenomenon is discussed in greater detail in Appendix B.

III. THEORY

A. Equilibrium argument for the temperature difference

In order to gain intuition about the surprising results concerning the temperature of both phases, we provide an intuitive argument grounded on an equilibrium description. Assuming the system remains close to equilibrium, we will for now utilize equilibrium results for the pressure to infer the possible temperature difference between the two phases that are slightly out of equilibrium.

Consider a coexistence between a liquid and a solid of hard disks *at equilibrium*. For hard disks, the pressure can be directly related to the contact value g^+ of the pair correlation function [96]:

$$p^{eq}(\phi, T, \phi g^+) = \frac{4\phi}{\sigma^2 \pi} T(1 + 2\phi g^+). \tag{5}$$

Note that even in equilibrium, we still define T as the average kinetic energy of a particle (see Eq. (3)). The constraint of mechanical equilibrium between the solid and the liquid phase can therefore be written as:

$$\phi_s T(1 + 2\phi_s g_s^+) = \phi_l T(1 + 2\phi_l g_l^+), \tag{6}$$

where g_s^+ and g_l^+ are the equilibrium pair correlation function at contact in the solid and in the liquid respectively. Note that the temperature T is the same for both phases, as we are considering an equilibrium system. Since $\phi_s > \phi_l$, it follows from Eqs. (6) that:

$$\phi_s g_s^+ < \phi_l g_l^+. \tag{7}$$

Moreover, the pressure of a hard-disk system is directly connected to the rate of collisions [96], leading to the Enskog expression for the collision frequency ω [97]:

$$\omega(T, \phi g^+) = 8\phi g^+ \sqrt{T/\sigma^2 \pi m}, \tag{8}$$

which holds exactly in equilibrium. We will later check the validity of this assumption, especially in the solid. This implies from Eq. (7) and (8) that the collision frequency in the solid is lower than in the liquid at coexistence:

$$\omega(T, \phi_s g_s^+) < \omega(T, \phi_l g_l^+). \tag{9}$$

In other words, the increase in density in the solid is compensated by a decrease in the collision frequency, such that the momentum exchange rate—or equivalently, the pressure—remains the same in both the liquid and the solid phases. We now assume that, close to equilibrium, the collision frequency in the coexisting liquid is still higher than in the solid. Under this approximation, in systems where energy is dissipated during collisions, the liquid phase is expected to be colder than in the coexisting solid. The same argument suggests a higher temperature in the coexisting liquid than in the solid when energy is injected during collisions. However, outside the coexistence region, the collision rate increases monotonically with density, causing temperature to decrease with density for dissipative collisions and increase when energy is injected at collision. This contrast between inside and outside the coexistence region explains the non-monotonic trend of the energy in both models shown in Fig. 1.

In this argument, we assumed that the non-equilibrium systems we consider here can be regarded as small perturbations to an equilibrium system, such that g^+ and the temperature of the system are only weakly affected by the introduction of non-equilibrium effects. Although

this equilibrium picture provides an intuitive argument for the expected behavior of the temperature difference, it leads to an internal inconsistency, where we use the assumption of thermal equilibrium to show the emergence of a temperature difference. In the next section, we explicitly take the temperature difference between the two phases into account in our analysis to derive it in a consistent way.

B. Non-equilibrium derivation of the temperature difference

We now take into account the non-equilibrium nature of our system. Assuming that velocities follow a Gaussian distribution and are uncorrelated before collisions, we find that the pressure p in either phase can be written as (see Appendix A):

$$p(\phi, T, \phi g^+) = \frac{4\phi}{\sigma^2 \pi}\left[T + \phi g^+\left((1+\alpha)T + 2\Delta\sqrt{\pi m T}\right)\right], \tag{10}$$

where we still find the ideal contribution and the virial contribution proportional to $(1+\alpha)T$ which represents momentum redistribution due to particle interactions. A new term proportional to Δ emerges from non-equilibrium velocity injection during collisions [98].

The steady state temperature arises from a balance between dissipation and energy injection [83]. Under the same assumptions as for the pressure, it can be shown that (see Appendix C):

$$\frac{\omega(T, \phi g^+)}{2}\left(m\Delta^2 + \alpha\Delta\sqrt{\pi m T} - (1-\alpha^2)T\right) - 2\gamma(T - T_b) = 0. \tag{11}$$

The first term of Eq. (11) represents the rate of energy change due to collisions, with the expression in parentheses describing the average energy change per collision. The second term accounts for energy exchange with the thermal bath. A crucial consequence of Eq. (11) is that the temperature depends on the density only through the frequency of collision. Therefore (far from the solid-liquid interface and when $\gamma \neq 0$) the temperatures of the coexisting phases can be assumed to depend solely on their respective values of ϕg^+.

This approach assumes that the velocity distribution remains approximately Gaussian and that velocities are uncorrelated during collisions. Together, these assumptions lead directly to Enskog's formula for the collision frequency (Eq. (8)), which we apply here. However, since we are interested in dense fluids and solids that, in principle, lie beyond the domain where Enskog theory applies, it is essential to test these assumptions. To this end, in Fig. 2a) and c), we compare measured temperatures to theoretical predictions for both the $\Delta + \gamma$ model and the GLM, respectively. These predictions were obtained using direct measurements of g^+ and the numerically calculated root of Eq. (11). Overall, the theory agrees

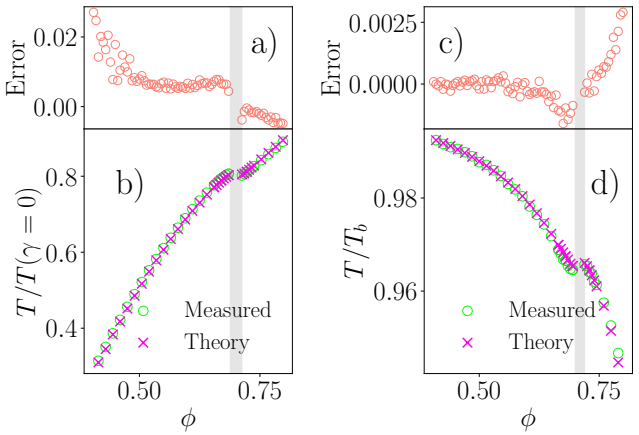

FIG. 2. Comparison between kinetic theory predictions and measured values of temperature. Panels a) and b) show the temperature predicted by kinetic theory (using measured values of g^+) compared to the directly measured temperature for the $\Delta + \gamma$ model. The Error is calculated as $(T_{\text{measured}} - T_{\text{theory}})/T_{\text{theory}}$. Panels c) and d) present the same comparison for the GLM. Both models are simulated utilizing the same parameters as in Fig.1.

well with numerical data, as demonstrated by the errors, see Fig. 2b) and d). Notably, for the $\Delta + \gamma$ model, the theory underperforms in the dilute limit due to an absorbing phase transition near $\phi \simeq 0.25$, where molecular chaos significantly breaks down [73, 99]. In contrast, the GLM behaves as expected: the theory is accurate at low densities but becomes less reliable as the packing fraction is increased. It may seem surprising that Enskog's theory, often considered valid only in the dilute limit, performs well here, even under non-equilibrium steady states. For instance, the theory is known to inaccurately predict transport coefficients, such as viscosity, in dense fluids [100] as these predictions are highly sensitive to collective effects and long-time tails [100] that Enskog's framework cannot capture. However, quantities such as the collision frequency that depend solely on the local environment are less affected by these non-local features. Based on these results, we conclude that the kinetic theory can be trusted to accurately predict temperatures within the parameter region studied ($\alpha > 0.95$).

The results presented in Fig. 2, show that the theory predicts well the non-monotonicity of the temperature. However, it requires measuring the values of g^+. While equilibrium predictions [100] proved to be good approximations for driven dissipative systems [73, 101–103], we will demonstrate that we can make useful predictions about the temperatures of both phases in the coexistence region of non-equilibrium hard disk systems without resorting to this approximation or relying on any equation of state.

Having tested the validity of our approximations as a first step, we note that mechanical stability still requires the

equality of pressure of both phases:

$$p(\phi_s, T_s, \phi_s g_s^+) = p(\phi_l, T_l, \phi_l g_l^+). \tag{12}$$

For simplicity, we assumed flat interfaces between the phases, avoiding the need to account for Laplace pressure and other interfacial stresses [104], which could influence the temperatures of each phase. The key insight is that energy change at collision implies that the density dependence of energy arises solely from the collision frequency, which in the Enskog approximation depends on density only through ϕg^+ (Eq. (8)). This means that ϕg^+ can be found if the temperature is known. Indeed, we can isolate ϕg^+ in the equation for the temperature Eq. (11) by inserting ω defined in Eq. (8) into it:

$$\phi g^+ \equiv \mathcal{G}(T) = \frac{\sigma\gamma\sqrt{\pi m}(T - T_b)}{2\sqrt{T}(m\Delta^2 + \alpha\Delta\sqrt{\pi m T} - (1-\alpha^2)T)}. \tag{13}$$

This allows us to eliminate the dependence on ϕg^+ in the pressure Eq. (12):

$$p(\phi_s, T_s, \mathcal{G}(T_s)) = p(\phi_l, T_l, \mathcal{G}(T_l)). \tag{14}$$

By eliminating ϕg^+, the pressure now explicitly depends only linearly on the density:

$$p(\phi, T, \mathcal{G}(T)) = \phi\tilde{p}(T, \mathcal{G}(T)) \tag{15}$$

where $\tilde{p}$ is defined as:

$$\tilde{p}(T, \mathcal{G}(T)) = \frac{\sigma^2\pi}{4}\frac{p}{\phi}, \tag{16}$$

which does not depend on ϕ. Finally, using mechanical equilibrium (see Eq. (14)) between phases and $\phi_s > \phi_l$, we find a non-equilibrium criterion:

$$\tilde{p}(T_s, \mathcal{G}(T_s)) < \tilde{p}(T_l, \mathcal{G}(T_l)). \tag{17}$$

Eq. (17) allows us to determine which phase is hotter based on $\mathcal{G}$, without needing to know an equation of state or g^+. For instance, if $\tilde{p}(T)$ is a continuous and increasing function of T, then Eq. (17) implies $T_s < T_l$. However, if $\tilde{p}$ is non-monotonic, the temperature comparison becomes more complex.

C. Hotter or Colder solid?

We first focus on the $\Delta + \gamma$ model ($T_b = 0$). In this model, $\tilde{p}$ is a continuous and monotonically increasing function of the physically accessible granular temperatures (see Appendix D). Consequently, from Eq. (17), we find that:

$$T_s^{\Delta+\gamma} < T_l^{\Delta+\gamma}. \tag{18}$$

As confirmed by our simulations, the temperature of the solid is predicted to be lower than that of the liquid, regardless of the parameters $\Delta > 0$ and $\gamma > 0$. Note that this theory still assumes molecular chaos and a Gaussian velocity distribution, therefore it should only be trusted near equilibrium conditions.

The theory for the GLM ($\Delta = 0$) is more intricate than that of the $\Delta + \gamma$ model. For this model, we obtain (see Appendix E):

$$\tilde{p}^{\mathrm{GLM}}(\tilde{T}) = T_b\tilde{T}\left(1 + \Lambda(1-\tilde{T})\tilde{T}^{-3/2}\right), \tag{19}$$

with:

$$\tilde{T} = T/T_b \quad \text{and} \quad \Lambda = \frac{\gamma\sigma\sqrt{\pi m/T_b}}{2(1-\alpha)} > 0. \tag{20}$$

Λ is a dimensionless parameter such that, at the Gaussian level, $\Lambda \to \infty$ corresponds to the equilibrium limit. Since the thermal bath is the only source of energy injection, the physical temperatures are constrained by $\tilde{T} < 1$.

For $\Lambda > 1$, $\tilde{p}$ is continuous and decreasing for $\tilde{T} < 1$, leading to the result:

$$T_l^{\mathrm{GLM}} < T_s^{\mathrm{GLM}} \text{ when } \Lambda > 1. \tag{21}$$

This explains the outcome observed in Fig. 1, where the solid was found to be hotter than the liquid in the GLM (with $\Lambda \simeq 10^2$).

However, in the strongly non-equilibrium case where $\Lambda < 1$, unlike the $\Delta + \gamma$ model, $\tilde{p}$ is not monotonically increasing, complicating the analysis. Nevertheless, we saw in Appendix B that for these small Λ the liquid-solid transition was most likely always continuous (i.e. without phase coexistence).

IV. DISCUSSION

Our investigations have shown that, in a granular system, the solid phase in a solid-liquid coexistence can indeed be hotter than the liquid. A heuristic, equilibrium-based argument for this counterintuitive result is that, at coexistence, the collision frequency in the solid phase is lower than in the liquid phase. Therefore, in systems where energy is dissipated through collisions, it is natural to expect the solid to be hotter than the liquid, even if the former is denser than the latter.

Although these heuristic arguments provide an intuitive explanation for our findings, they start from an equilibrium assumption, with constant temperature throughout the system, rendering them inconsistent when used to predict temperature differences. The more rigorous analysis in Sec. III overcomes this limitation by explicitly incorporating the temperature difference between the two phases.

In developing the theory, we made certain assumptions that may not strictly hold out of equilibrium. Specifically, we assumed molecular chaos and a Gaussian velocity distribution, which can easily break down [98, 105–108], particularly in the solid phase. However, we show

that close to equilibrium, the predictions from kinetic theory works exceptionally well even in the solid. We also showed in Ref. 72 that the theory still works even in a binary mixture where energy equipartition between small and large disks does not hold. Extensions beyond the Gaussian assumption are possible [98, 105, 109, 110] but fall outside the scope of this article.

The models we introduced are simplified compared to realistic granular experiments, such as quasi-2D vibrated granular matter. As a first step, the analysis performed on the two limiting models can be extended to the full system with $\Delta \neq 0$ and $T_b \neq 0$. However, nothing too surprising emerges from this extension: either the bath or Δ dominates the energy injection, and the temperature difference follows. In more realistic systems of quasi-2D vibrated monodisperse granular beads, the dense phase was always found to be colder than the dilute one due to effects not accounted for in our simplified 2D model: bistability of the grain-plate dynamics [67, 111], strong vertical confinement [63], dynamical instabilities [48, 50], non-homogeneous energy injection [58] among others. While our study has the merit of showing that the temperature difference commonly observed in granular system cannot be solely explained by dissipative collision, a crucial next step would be to incorporate these factors into our model to gain a better understanding of what governs the temperature difference between the two phases. Conversely, from an experimental standpoint, it would be interesting to optimize the realistic parameters of the quasi-2D system to get as close as possible to the effective GLM, and to investigate whether it is feasible to obtain a monodisperse granular solid that is hotter than its coexisting liquid. We also note that in multicomponent hard disk mixtures, where a variety of crystal and quasi-crystal structures can form [74, 112–114], a granular solid was observed to be hotter than the liquid in a realistic quasi-2D vibrated system. This is because collisions between some species are geometrically impossible in a perfect crystal but not in the liquid, reducing a source of dissipation only in the dense phase [72].

In active matter, motility-induced phase separation can be realized by self-propelled macroscopic agents undergoing dissipative collisions [6, 46]. Since the phase separation in these systems arises from a dynamical instability associated with a reduction in effective self-propulsion—and consequently in effective temperature—as the system's density increases, it is unlikely that the effect we have identified plays a significant role in these cases.

Additionally, our theory assumes the solid-liquid transition is discontinuous. However, for the GLM, we found that this is not always the case (see Appendix B). This could be attributed to the softening of the effective interaction due to dissipative collisions [115–117]. Indeed, particles with potentials softer than hard-core repulsion are known to undergo the standard two steps Kosterlitz-Thouless-Halperin-Nelson-Young melting transition [118–122] from a solid to a hexatic and then from a hexatic to a liquid phase, which both occur continuously [123, 124]. Lastly, the question of hexatic order in these systems is of significant interest and was not addressed in this study. Recent work has shown that crystals formed in the $\Delta + \gamma$ model exhibit translational long-range order due to hyperuniformity [86, 125–127], in striking violation of the Mermin-Wagner theorem. It would be interesting to explore the impact of temperature difference and translational long-range order on the nature of the melting of granular crystals.

ACKNOWLEDGMENTS

AP acknowledges the Agence Nationale de la Recherche (ANR), Grant ANR-21-CE06-0039, which provided funding for this research. The data that support the findings of this study are available from the corresponding author upon reasonable request.

Appendix A: Determination of the pressure

The typical method for obtaining the pressure at equilibrium is through the virial pressure formula. Out of equilibrium, pressure can either be derived from the Boltzmann equation or through a method analogous to that used in equilibrium. In this work, we follow the latter approach. The pressure p in 2D systems interacting through 2-body forces can be written as [128]:

$$p = \frac{4\phi}{\sigma^2\pi}\left(T - \frac{1}{2N}\sum_{i<j}^{N}\langle \boldsymbol{r}_{ij}\cdot\boldsymbol{F}_{ij}\rangle\right), \tag{A1}$$

where $\boldsymbol{F}_{ij}$ is the force between particles i and j. Similar to equilibrium systems, the Langevin thermostat only contributes to the ideal part of the pressure and does not affect the virial term, which arises from momentum exchanges between particles. Notably, Eq. (A1) can also be derived from a direct evaluation of the momentum exchange at a boundary.

The force between particles i and j can be derived from the collision rule Eq. (1) using $m\mathrm{d}\boldsymbol{v}_i/\mathrm{d}t = \boldsymbol{F}_{ij}$:

$$\boldsymbol{F}_{ij} = -m\left(\frac{1+\alpha}{2}|\boldsymbol{v}_{ij}\cdot\hat{\boldsymbol{\sigma}}_{ij}| + \Delta\right)\hat{\boldsymbol{\sigma}}_{ij}\delta(t - t_{ij}^{\mathrm{coll}}), \tag{A2}$$

with t_{ij}^{coll} the time of collision between particle i and j. Eq. (A1) can be simplified using Enskog's collision frequency (C6), the expression of the instantaneous force (A2) and the collisional average defined in Eq. (C5):

$$\begin{aligned} p &= \frac{4\phi}{\sigma^2\pi}\left[T + \frac{m\sigma\omega(T,\phi g^+)}{4}\left\langle\frac{1+\alpha}{2}|\boldsymbol{v}_{ij}\cdot\hat{\boldsymbol{\sigma}}_{ij}| + \Delta\right\rangle_{\mathrm{coll}}\right] \\ &= \frac{4\phi}{\sigma^2\pi}\left[T + \phi g^+\sqrt{T}\left((1+\alpha)\sqrt{T} + 2\sqrt{\pi m}\Delta\right)\right], \end{aligned} \tag{A3}$$

which coincides with Eq. (10) in the main text.

Note that from the average we can also obtain an expression for the microscopic running pressure used in the Event-Driven simulations to measure the pressure:

$$p_{\text{micro}} = \frac{NT}{L_x L_y} + \frac{m\sigma}{2L_x L_y t} \sum_{\text{coll-ij}} \left(\frac{1+\alpha}{2} \left(\boldsymbol{v}_{ij} \cdot \hat{\boldsymbol{\sigma}}_{ij} \right) + \Delta \right), \tag{A4}$$

where t is the time simulation window and the sum is over all collisions.

Appendix B: From discontinuous to continuous liquid-solid phase transition

The liquid-solid phase transition in the GLM can become continuous under certain conditions. In the equilibrium limit $\Lambda \to \infty$, the model appears to transition from the liquid to the solid phase (most likely an hexatic phase) in a discontinuous manner, as shown in Fig. 3a). This is consistent with the known behavior of equilibrium hard-disks [87]. However, as Λ decreases and dissipation becomes more significant, the transition appears to become continuous, with no Mayer-Wood loop [94]—indicative of strong, finite-sized interfacial effects—observed in the pressure. This behavior is reminiscent of the classical two-step Kosterlitz-Thouless-Halperin-Nelson-Young (KTHNY) transition, where the liquid-to-hexatic transition is continuous. It has been shown that systems interacting with soft potentials —for example, $V(r) \propto r^n$ with $n < 6$ — can follow the KTHNY scenario in transitioning from the solid to the liquid phase [123, 124].

In our system, the observed change in behavior as dissipation increases may be explained by an effective softening of the hard-disk potential [115–117]. However, further studies are necessary to fully understand the mechanisms underlying this change in the nature of the transition.

Interestingly, a loop in the energy is consistently observed in Fig. 3b), regardless of whether the transition is continuous or discontinuous. This suggests that even in the absence of a first-order phase transition, the structural changes associated with the transition to the solid phase lead to an increase in temperature around the transition point.

We finally note that a change from continuous to discontinuous in the liquid-solid transition was also observed in an experimental vibrated granular gas in Ref. [75, 76] upon changing driving parameters and in Ref. [60] while changing the properties of the grains.

Appendix C: Determination of the temperature

We define the instantaneous energy of the system as $E = m/2 \sum_{i=1}^{N} \boldsymbol{v}_i^2$. From the collision rule, the energy change during a collision is given by:

$$\Delta E = m\Delta^2 + \alpha m (\boldsymbol{v}_{ij} \cdot \hat{\boldsymbol{\sigma}}_{ij}) \Delta - m \frac{1-\alpha^2}{4} (\boldsymbol{v}_{ij} \cdot \hat{\boldsymbol{\sigma}}_{ij})^2. \tag{C1}$$

The evolution of the temperature in the system is then given by:

$$\frac{\mathrm{d}T}{\mathrm{d}t} = \frac{\omega}{2} \langle \Delta E \rangle_{\text{coll}} - 2\gamma (T - T_b), \tag{C2}$$

where ω is the collision frequency and $\langle \dots \rangle_{\text{coll}}$ is an average over collisions defined from the Boltzmann equation as:

$$\langle A(\boldsymbol{v}_{ij}, \hat{\boldsymbol{\sigma}}_{ij}) \rangle_{\text{coll}} = \frac{\int d\boldsymbol{v}_i \int d\boldsymbol{v}_j \int d\hat{\boldsymbol{\sigma}}_{ij} \Theta(-\boldsymbol{v}_{ij} \cdot \hat{\boldsymbol{\sigma}}_{ij}) |\boldsymbol{v}_{ij} \cdot \hat{\boldsymbol{\sigma}}_{ij}| A(\boldsymbol{v}_{ij}, \hat{\boldsymbol{\sigma}}_{ij}) f^{(2)}(\boldsymbol{v}_i, \boldsymbol{v}_j, \hat{\boldsymbol{\sigma}}_{ij})}{\int d\boldsymbol{v}_i \int d\boldsymbol{v}_j \int d\hat{\boldsymbol{\sigma}}_{ij} \Theta(-\boldsymbol{v}_{ij} \cdot \hat{\boldsymbol{\sigma}}_{ij}) |\boldsymbol{v}_{ij} \cdot \hat{\boldsymbol{\sigma}}_{ij}| f^{(2)}(\boldsymbol{v}_i, \boldsymbol{v}_j, \hat{\boldsymbol{\sigma}}_{ij})}. \tag{C3}$$

Θ is the Heaviside function that ensures only particles approaching each other are considered, $|\boldsymbol{v}_{ij} \cdot \hat{\boldsymbol{\sigma}}_{ij}|$ can be interpreted as a flux times a cross-section for the hard-disks interaction, and $f^{(2)}(\boldsymbol{v}_1, \boldsymbol{v}_2, \boldsymbol{\sigma}_{ij})$ is the pair distribution function of the velocities. Assuming molecular chaos with Enskog's extension, we simplify the two points velocity distribution:

$$f^{(2)}(\boldsymbol{v}_i, \boldsymbol{v}_j, \hat{\boldsymbol{\sigma}}_{ij}) \simeq g^{+} f(\boldsymbol{v}_i) f(\boldsymbol{v}_j), \tag{C4}$$

where g^{+} is the pair correlation function at contact and $f(\boldsymbol{v})$ the distribution of velocity assumed to be a gaussian. These assumptions of molecular chaos and gaussianity of the velocity distribution let us approximate Eq. C3 to the following form in 2D:

$$\langle A \rangle_{\text{coll}} = \frac{\int_0^{\infty} \mathrm{d}v \int_{-\pi/2}^{\pi/2} \mathrm{d}\theta \cos(\theta) A(v, \theta) \frac{mv^2}{2T} e^{-\frac{1}{2}\frac{mv^2}{2T}}}{2\sqrt{\frac{\pi T}{m}}}. \tag{C5}$$

These assumptions also lead to the Enskog expression for the collision frequency that we used in the main text:

$$\omega(T, \phi g^{+}) = \langle |\boldsymbol{v}| \rangle / l(\phi) = 8\phi g^{+} \sqrt{T/(\pi m)}/\sigma. \tag{C6}$$

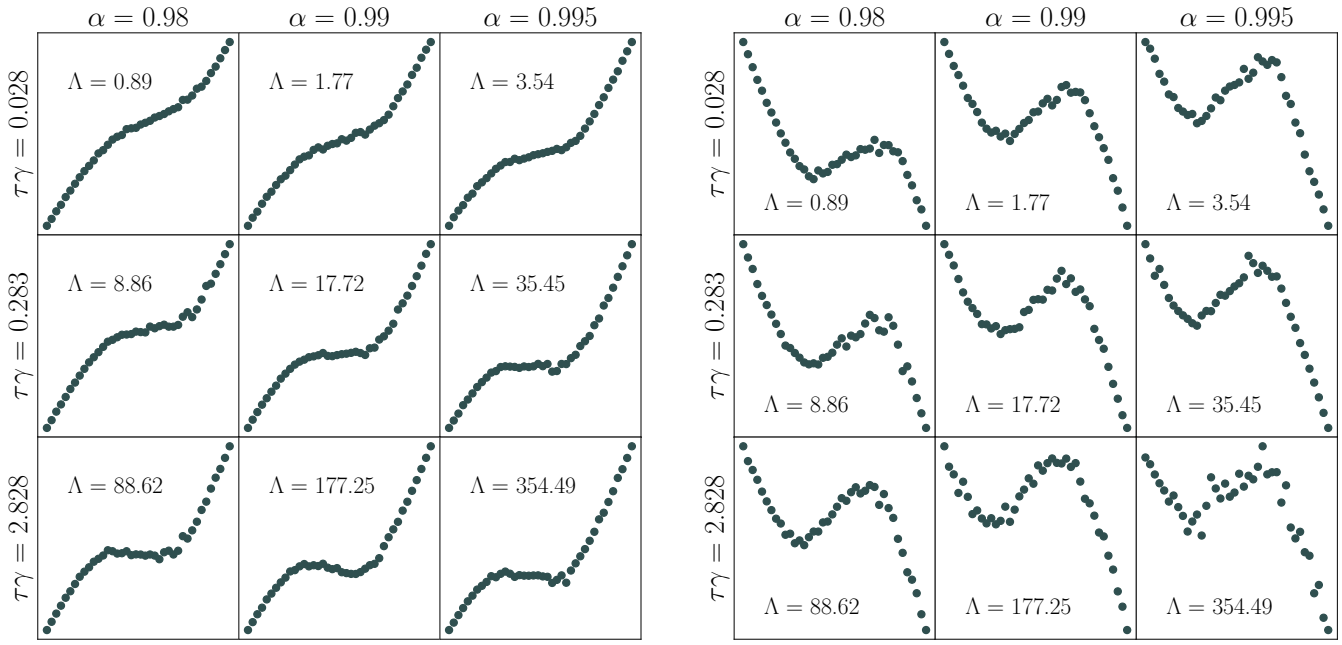

(a) Pressure

(b) Energy

FIG. 3. a) Evolution of pressure (in arbitrary units) as a function of density for the GLM, for various γ and α ($\tau = \sqrt{m\sigma^2/T_b}$). b) Same as in a), but for the energy instead of the pressure (in arbitrary units). $N = 10^4$.

Eq. (C6) can be equivalently obtained from the integration of the loss term in the Boltzmann equation. Indeed, this integral computes the rate at which a particle of *any* velocity changes velocity due to collision, which is by definition the collision frequency [129].

Eqs. (C5) and (C1) lead to the following equation for the steady state temperature used in the main text:

$$0 = \frac{\omega}{2}(m\Delta^2+\alpha\Delta\sqrt{\pi mT}-T(1-\alpha^2))-2\gamma(T-T_b). \quad \text{(C7)}$$

Appendix D: Details concerning the $\Delta+\gamma$ model

In the $\Delta+\gamma$ model, $T_b = 0$, therefore $\mathcal{G}$ reduces to:

$$\phi g^+ \equiv \mathcal{G}^{\Delta+\gamma} = \frac{\sigma\gamma\sqrt{\pi m}T}{2\sqrt{T}(m\Delta^2+\alpha\Delta\sqrt{\pi mT}-(1-\alpha^2)T)}, \quad \text{(D1)}$$

and $\tilde{p}^{\Delta+\gamma}$ reads:

$$\tilde{p}^{\Delta+\gamma} = T + \mathcal{G}^{\Delta+\gamma}(T)\left((1+\alpha)T+2\Delta\sqrt{\pi mT}\right). \quad \text{(D2)}$$

In order to know whether T_s is larger or smaller than T_l using the inequality $\tilde{p}^{\Delta+\gamma}(T_s) < \tilde{p}^{\Delta+\gamma}(T_l)$, we must know the variations of $\tilde{p}$. Direct computation of the derivative of $\tilde{p}^{\Delta+\gamma}$ with respect to T leads to:

$$\begin{aligned}\frac{\mathrm{d}\tilde{p}^{\Delta+\gamma}}{\mathrm{d}T} = 1 &+ \left(1+\alpha+\Delta\sqrt{\pi m/T}\right)\mathcal{G}^{\Delta+\gamma} \\ &+ \left((1+\alpha)T+2\Delta\sqrt{\pi mT}\right)\frac{\mathrm{d}\mathcal{G}^{\Delta+\gamma}}{\mathrm{d}T},\end{aligned} \quad \text{(D3)}$$

using $m\Delta^2+\alpha\Delta\sqrt{\pi mT}-(1-\alpha^2)T = 4\gamma T/\omega > 0$ (Eq. (C7)), we can show that $\frac{\mathrm{d}\mathcal{G}^{\Delta+\gamma}}{\mathrm{d}T} > 0$ and $\mathcal{G}^{\Delta+\gamma} > 0$ from which we obtain that $\mathrm{d}\tilde{p}^{\Delta+\gamma}/\mathrm{d}T > 0$. This proves that $\tilde{p}^{\Delta+\gamma}$ is a continuous and increasing function of the relevant temperatures.

Using the monotonous increase of $\tilde{p}^{\Delta+\gamma}$, we finally arrive to our result:

$$\tilde{p}^{\Delta+\gamma}(T_s^{\Delta+\gamma}) < \tilde{p}^{\Delta+\gamma}(T_l^{\Delta+\gamma}) \Rightarrow T_s^{\Delta+\gamma} < T_l^{\Delta+\gamma}, \quad \text{(D4)}$$

which shows that the solid is colder than the liquid at coexistence in the $\Delta+\gamma$ model.

Appendix E: Details concerning the GLM

In the GLM, $\Delta = 0$, therefore $\mathcal{G}$ simplifies to:

$$\phi g^+ \equiv \mathcal{G}^{\mathrm{GLM}} = \frac{\sigma\gamma\sqrt{\pi m}(T_b-T)}{2(1-\alpha^2)T^{3/2}}, \quad \text{(E1)}$$

and $\tilde{p}^{\mathrm{GLM}}$ reads:

$$\begin{aligned}\tilde{p}^{\mathrm{GLM}} &= T\left(1+\mathcal{G}^{\mathrm{GLM}}(T)(1+\alpha)\right) \\ &= T_b\tilde{T}\left(1+\Lambda(1-\tilde{T})\tilde{T}^{-3/2}\right),\end{aligned} \quad \text{(E2)}$$

with $\tilde{T} = T/T_b$ and $\Lambda = \frac{\gamma\sigma\sqrt{\pi m/T_b}}{2(1-\alpha)} > 0$ a dimensionless parameter such that, when molecular chaos holds and velocities follow a gaussian distribution, $\Lambda \to \infty$ corresponds to an equilibrium limit.

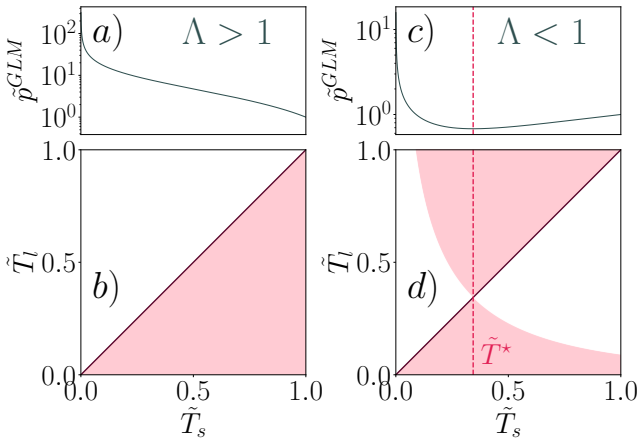

FIG. 4. Typical behavior of $\tilde{p}^{\mathrm{GLM}}$ and $\tilde{p}^{\mathrm{GLM}}(T_s) < \tilde{p}^{\mathrm{GLM}}(T_l)$ for $\Lambda > 1$ and $\Lambda < 1$. a) and c) Evolution of $\tilde{p}^{\mathrm{GLM}}$ as a function of $\tilde{T}$. For $\Lambda > 1$, $\tilde{p}$ is purely decreasing while for $\Lambda > 1$, $\tilde{p}^{\mathrm{GLM}}$ has a change of variation at $\tilde{T}^\star$. b) and d) The corresponding regions which verify $\tilde{p}^{\mathrm{GLM}}(T_s) < \tilde{p}^{\mathrm{GLM}}(T_l)$. The shaded regions are the region in which the inequality holds. For $\Lambda > 1$, we obtain $\tilde{T}_s > \tilde{T}_l$. However, for $\Lambda < 1$, both scenario are possible. Hence, determining whether $\tilde{T}_s > \tilde{T}_l$ requires estimates for ϕg^+.

Since the bath is the only source of energy injection in the system, physical temperatures must respect $T < T_b$ and hence $\tilde{T} < 1$. We can therefore restrict our attention to the behavior of $\tilde{p}^{\mathrm{GLM}}$ at $\tilde{T} < 1$. In order to know whether T_s is larger or smaller than T_l using the inequality $\tilde{p}^{\mathrm{GLM}}(T_s^{\mathrm{GLM}}) < \tilde{p}^{\mathrm{GLM}}(T_l^{\mathrm{GLM}})$, we must know the variations of $\tilde{p}^{\mathrm{GLM}}$. Direct computation of the derivative of $\tilde{p}^{\mathrm{GLM}}$ with respect to T leads to:

$$\frac{\mathrm{d}\tilde{p}^{\mathrm{GLM}}}{\mathrm{d}T} = T_b \left(1 - \frac{\Lambda}{2}(1+\tilde{T})\tilde{T}^{-3/2}\right). \tag{E3}$$

Eq. (E3) implies that $\tilde{p}^{\mathrm{GLM}}$ is decreasing from 0 to $\tilde{T}^\star$ and then increasing from $\tilde{T}^\star$ to ∞, where $\tilde{T}^\star$ is the unique real root of Eq. (E3) given by a third order polynomial in $\tilde{T}^{1/2}$:

$$2(\tilde{T}^\star)^{3/2} - \Lambda(1+\tilde{T}^\star) = 0. \tag{E4}$$

We now perform an asymptotic expansion around $\Lambda = 1$ where the solution $\tilde{T}^\star = 1$ of the polynomial Eq. (E4) is known:

$$\begin{aligned} \Lambda &= 1 + \varepsilon \\ \tilde{T}^\star &= 1 + \sum_{i=1}^{\infty} a_i \varepsilon^i. \end{aligned} \tag{E5}$$

Inserting Eq. (E5) in Eq. (E4) and solving order by order leads the following approximation for the root of Eq. (E3):

$$\tilde{T}^* = 1 + (\Lambda - 1) + \frac{1}{8}(\Lambda - 1)^2 + \mathcal{O}\left((\Lambda - 2)^3\right). \tag{E6}$$

For $\Lambda > 1$, as it is clear that the exact root $\tilde{T}^\star(\Lambda)$ is monotonically increasing, it must satisfies $\tilde{T}^\star > 1$, therefore, for the physically accessible temperatures ($\tilde{T} < 1$), $\tilde{p}^{\mathrm{GLM}}$ is decreasing which implies:

$$\begin{aligned} \tilde{p}^{\mathrm{GLM}}(T_s^{\mathrm{GLM}}) &< \tilde{p}^{\mathrm{GLM}}(T_l^{\mathrm{GLM}}) \\ \Downarrow\ \Lambda &> 1 \\ T_s^{\mathrm{GLM}} &> T_l^{\mathrm{GLM}}. \end{aligned} \tag{E7}$$

This behavior of $\tilde{p}^{\mathrm{GLM}}$ is exemplified in Fig. 4a) and the corresponding constraints on $\tilde{T}_s$ and $\tilde{T}_l$ are given by Fig. 4b) where the shaded area are the region in which the inequality Eq. (17) is verified.

In contrast, when $\Lambda < 1$, $\tilde{p}^{\mathrm{GLM}}$ changes from being decreasing to increasing at a value of $\tilde{T}^*$ between 0 and 1. Hence, the constraint on the pressure alone does not determine which phase is hotter. This is exemplified in Fig. 4c) and d). However in this limit, the system was typically always observed to crystallize via a continuous transition, rather than through a phase coexistence, in numerical simulations (see Appendix. B).

[1] Josiah Willard Gibbs. On the equilibrium of heterogeneous substances. American Journal of Science, 3(96):441–458, 1878.

[2] Michael E Cates and Julien Tailleur. Motility-induced phase separation. Annu. Rev. Condens. Matter Phys., 6(1):219–244, 2015.

[3] ME Cates and C Nardini. Active phase separation: new phenomenology from non-equilibrium physics. arXiv preprint arXiv:2412.02854, 2024.

[4] Friedrich Schlögl. Chemical reaction models for non-equilibrium phase transitions. Zeitschrift für physik, 253(2):147–161, 1972.

[5] Suvendu Mandal, Benno Liebchen, and Hartmut Löwen. Motility-induced temperature difference in coexisting phases. Physical review letters, 123(22):228001, 2019.

[6] Marjolein N Van Der Linden, Lachlan C Alexander, Dirk GAL Aarts, and Olivier Dauchot. Interrupted motility induced phase separation in aligning active colloids. Physical review letters, 123(9):098001, 2019.

[7] Michael E Cates, D Marenduzzo, I Pagonabarraga, and J Tailleur. Arrested phase separation in reproducing bacteria creates a generic route to pattern formation. Proceedings of the National Academy of Sciences, 107(26):11715–11720, 2010.

[8] Ethayaraja Mani and Hartmut Löwen. Effect of self-propulsion on equilibrium clustering. Physical Review E, 92(3):032301, 2015.

[9] Vasileios Prymidis, Harmen Sielcken, and Laura Filion. Self-assembly of active attractive spheres. Soft Matter,

11(21):4158–4166, 2015.

[10] Supriya Saha, Ramin Golestanian, and Sriram Ramaswamy. Clusters, asters, and collective oscillations in chemotactic colloids. Physical Review E, 89(6):062316, 2014.

[11] Benno Liebchen, Davide Marenduzzo, Ignacio Pagonabarraga, and Michael E Cates. Clustering and pattern formation in chemorepulsive active colloids. Physical review letters, 115(25):258301, 2015.

[12] Ricard Matas-Navarro, Ramin Golestanian, Tanniemola B Liverpool, and Suzanne M Fielding. Hydrodynamic suppression of phase separation in active suspensions. Physical Review E, 90(3):032304, 2014.

[13] Shashi Thutupalli, Delphine Geyer, Rajesh Singh, Ronojoy Adhikari, and Howard A Stone. Flow-induced phase separation of active particles is controlled by boundary conditions. Proceedings of the National Academy of Sciences, 115(21):5403–5408, 2018.

[14] Raphael Wittkowski, Adriano Tiribocchi, Joakim Stenhammar, Rosalind J Allen, Davide Marenduzzo, and Michael E Cates. Scalar φ 4 field theory for active-particle phase separation. Nature communications, 5(1):4351, 2014.

[15] Alexandre P Solon, Joakim Stenhammar, Michael E Cates, Yariv Kafri, and Julien Tailleur. Generalized thermodynamics of motility-induced phase separation: phase equilibria, laplace pressure, and change of ensembles. New Journal of Physics, 20(7):075001, 2018.

[16] Ahmad K Omar, Hyeongjoo Row, Stewart A Mallory, and John F Brady. Mechanical theory of nonequilibrium coexistence and motility-induced phase separation. Proceedings of the National Academy of Sciences, 120(18):e2219900120, 2023.

[17] Fernando Caballero, Ananyo Maitra, and Cesare Nardini. Interface dynamics of wet active systems. arXiv preprint arXiv:2409.02288, 2024.

[18] Marc Besse, Giordano Fausti, Michael E Cates, Bertrand Delamotte, and Cesare Nardini. Interface roughening in nonequilibrium phase-separated systems. Physical Review Letters, 130(18):187102, 2023.

[19] Xia-qing Shi, Giordano Fausti, Hugues Chaté, Cesare Nardini, and Alexandre Solon. Self-organized critical coexistence phase in repulsive active particles. Physical Review Letters, 125(16):168001, 2020.

[20] Sudipta Pattanayak, Shradha Mishra, and Sanjay Puri. Ordering kinetics in the active model b. Physical Review E, 104(1):014606, 2021.

[21] Giordano Fausti, Michael E Cates, and Cesare Nardini. Statistical properties of microphase and bubbly phase-separated active fluids. Physical Review E, 110(4):L042103, 2024.

[22] Elsen Tjhung, Cesare Nardini, and Michael E Cates. Cluster phases and bubbly phase separation in active fluids: reversal of the ostwald process. Physical Review X, 8(3):031080, 2018.

[23] Claudio B Caporusso, Pasquale Digregorio, Demian Levis, Leticia F Cugliandolo, and Giuseppe Gonnella. Motility-induced microphase and macrophase separation in a two-dimensional active brownian particle system. Physical Review Letters, 125(17):178004, 2020.

[24] Ahmad K Omar, Zhen-Gang Wang, and John F Brady. Microscopic origins of the swim pressure and the anomalous surface tension of active matter. Physical Review E, 101(1):012604, 2020.

[25] Luke Langford and Ahmad K Omar. The mechanics of nucleation and growth and the surface tensions of active matter. arXiv preprint arXiv:2407.06462, 2024.

[26] Adam Patch, Daniel M Sussman, David Yllanes, and M Cristina Marchetti. Curvature-dependent tension and tangential flows at the interface of motility-induced phases. Soft matter, 14(36):7435–7445, 2018.

[27] Ruben Zakine, Yongfeng Zhao, Miloš Knežević, Adrian Daerr, Yariv Kafri, Julien Tailleur, and Frédéric van Wijland. Surface tensions between active fluids and solid interfaces: Bare vs dressed. Physical Review Letters, 124(24):248003, 2020.

[28] Shin-ichi Sasa and Naoko Nakagawa. Non-equilibrium phase coexistence in boundary-driven diffusive systems. arXiv preprint arXiv:2407.12353, 2024.

[29] Naoko Nakagawa and Shin-ichi Sasa. Liquid-gas transitions in steady heat conduction. Physical review letters, 119(26):260602, 2017.

[30] Akira Yoshida, Naoko Nakagawa, and Shin-ichi Sasa. Heat-induced liquid hovering in liquid-gas coexistence under gravity. Physical Review Letters, 133(11):117101, 2024.

[31] Michikazu Kobayashi, Naoko Nakagawa, and Shin-ichi Sasa. Control of metastable states by heat flux in the hamiltonian potts model. Physical Review Letters, 130(24):247102, 2023.

[32] Shin-ichi Sasa, Naoko Nakagawa, Masato Itami, and Yohei Nakayama. Stochastic order parameter dynamics for phase coexistence in heat conduction. Physical Review E, 103(6):062129, 2021.

[33] Vincent Ouazan-Reboul, Jaime Agudo-Canalejo, and Ramin Golestanian. Self-organization of primitive metabolic cycles due to non-reciprocal interactions. Nature Communications, 14(1):4496, 2023.

[34] Michel Fruchart, Ryo Hanai, Peter B Littlewood, and Vincenzo Vitelli. Non-reciprocal phase transitions. Nature, 592(7854):363–369, 2021.

[35] Lorenz Butzhammer, Simeon Völkel, Ingo Rehberg, and Kai Huang. Pattern formation in wet granular matter under vertical vibrations. Physical Review E, 92(1):012202, 2015.

[36] Istafaul Haque Ansari, Nicolas Rivas, and Meheboob Alam. Phase-coexisting patterns, horizontal segregation, and controlled convection in vertically vibrated binary granular mixtures. Physical Review E, 97(1):012911, 2018.

[37] Yu-Jen Chiu and Ahmad K Omar. Phase coexistence implications of violating newton's third law. The Journal of chemical physics, 158(16), 2023.

[38] Hartmut Löwen. Inertial effects of self-propelled particles: From active brownian to active langevin motion. The Journal of chemical physics, 152(4), 2020.

[39] Lorenzo Caprini, Umberto Marini Bettolo Marconi, and Andrea Puglisi. Spontaneous velocity alignment in motility-induced phase separation. Physical review letters, 124(7):078001, 2020.

[40] Lorenzo Caprini and Umberto Marini Bettolo Marconi. Inertial self-propelled particles. The Journal of Chemical Physics, 154(2), 2021.

[41] Lorenzo Caprini, Rahul Kumar Gupta, and Hartmut Löwen. Role of rotational inertia for collective phenomena in active matter. Physical Chemistry Chemical Physics, 24(40):24910–24916, 2022.

[42] Yuta Kuroda, Hiromichi Matsuyama, Takeshi

Kawasaki, and Kunimasa Miyazaki. Anomalous fluctuations in homogeneous fluid phase of active brownian particles. Physical Review Research, 5(1):013077, 2023.

[43] Antonio Suma, Giuseppe Gonnella, Davide Marenduzzo, and Enzo Orlandini. Motility-induced phase separation in an active dumbbell fluid. Europhysics Letters, 108(5):56004, 2014.

[44] Lukas Hecht, Suvendu Mandal, Hartmut Löwen, and Benno Liebchen. Active refrigerators powered by inertia. Physical Review Letters, 129(17):178001, 2022.

[45] Lukas Hecht, Lorenzo Caprini, Hartmut Löwen, and Benno Liebchen. How to define temperature in active systems. arXiv preprint arXiv:2407.19281, 2024.

[46] Lorenzo Caprini, Davide Breoni, Anton Ldov, Christian Scholz, and Hartmut Löwen. Dynamical clustering and wetting phenomena in inertial active matter. Communications Physics, 7(1):343, 2024.

[47] Lukas Hecht, Iris Dong, and Benno Liebchen. Motility-induced coexistence of a hot liquid and a cold gas. Nature Communications, 15(1):3206, 2024.

[48] Dino Risso, Rodrigo Soto, and Marcelo Guzmán. Effective two-dimensional model for granular matter with phase separation. Physical Review E, 98(2):022901, 2018.

[49] James PD Clewett, Jack Wade, RM Bowley, Stephan Herminghaus, Michael R Swift, and Marco G Mazza. The minimization of mechanical work in vibrated granular matter. Scientific Reports, 6(1):28726, 2016.

[50] C Cartes, MG Clerc, and R Soto. van der waals normal form for a one-dimensional hydrodynamic model. Physical Review E—Statistical, Nonlinear, and Soft Matter Physics, 70(3):031302, 2004.

[51] Evgeniy Khain and Igor S Aranson. Hydrodynamics of a vibrated granular monolayer. Physical Review E—Statistical, Nonlinear, and Soft Matter Physics, 84(3):031308, 2011.

[52] Mederic Argentina, MG Clerc, and R Soto. Van der waals–like transition in fluidized granular matter. Physical review letters, 89(4):044301, 2002.

[53] Stephan Herminghaus and Marco G Mazza. Phase separation in driven granular gases: exploring the elusive character of nonequilibrium steady states. Soft matter, 13(5):898–910, 2017.

[54] Evgeniy Khain, Baruch Meerson, and Pavel V Sasorov. Phase diagram of van der waals–like phase separation in a driven granular gas. Physical Review E—Statistical, Nonlinear, and Soft Matter Physics, 70(5):051310, 2004.

[55] Evgeniy Khain and Baruch Meerson. Oscillatory instability in a driven granular gas. Europhysics Letters, 65(2):193, 2004.

[56] J Javier Brey, V Buzón, MI García de Soria, and P Maynar. Stability analysis of the homogeneous hydrodynamics of a model for a confined granular gas. Physical Review E, 93(6):062907, 2016.

[57] Klaus Roeller, James PD Clewett, RM Bowley, Stephan Herminghaus, and Michael R Swift. Liquid-gas phase separation in confined vibrated dry granular matter. Physical Review Letters, 107(4):048002, 2011.

[58] Martial Noirhomme, Annette Cazaubiel, Eric Falcon, David Fischer, Yves Garrabos, Carole Lecoutre-Chabot, Sébastien Mawet, Eric Opsomer, Fabien Palencia, Salvatore Pillitteri, et al. Particle dynamics at the onset of the granular gas-liquid transition. Physical Review Letters, 126(12):128002, 2021.

[59] Martial Noirhomme, Annette Cazaubiel, Alexis Darras, Eric Falcon, David Fischer, Yves Garrabos, Carole Lecoutre-Chabot, Simon Merminod, Eric Opsomer, Fabien Palencia, et al. Threshold of gas-like to clustering transition in driven granular media in low-gravity environment. Europhysics Letters, 123(1):14003, 2018.

[60] Yuta Komatsu and Hajime Tanaka. Roles of energy dissipation in a liquid-solid transition of out-of-equilibrium systems. Physical Review X, 5(3):031025, 2015.

[61] Marcel G Clerc, Patricio Cordero, Jocelyn Dunstan, K Huff, Nicolás Mujica, Dino Risso, and Germán Varas. Liquid–solid-like transition in quasi-one-dimensional driven granular media. Nature Physics, 4(3):249–254, 2008.

[62] Li-Hua Luu, Gustavo Castillo, Nicolás Mujica, and Rodrigo Soto. Capillarylike fluctuations of a solid-liquid interface in a noncohesive granular system. Physical Review E—Statistical, Nonlinear, and Soft Matter Physics, 87(4):040202, 2013.

[63] Alexis Prevost, Paul Melby, David A Egolf, and Jeffrey S Urbach. Nonequilibrium two-phase coexistence in a confined granular layer. Physical Review E—Statistical, Nonlinear, and Soft Matter Physics, 70(5):050301, 2004.

[64] N Rivas, P Cordero, D Risso, and R Soto. Characterization of the energy bursts in vibrated shallow granular systems. Granular Matter, 14:157–162, 2012.

[65] Andreas Götzendorfer, Jennifer Kreft, Christof A Kruelle, and Ingo Rehberg. Sublimation of a vibrated granular monolayer: Coexistence of gas and solid. Physical review letters, 95(13):135704, 2005.

[66] Paul Melby, F Vega Reyes, Alexis Prevost, Rae Robertson, Pramukta Kumar, David A Egolf, and Jeffrey S Urbach. The dynamics of thin vibrated granular layers. Journal of Physics: Condensed Matter, 17(24):S2689, 2005.

[67] J. S. Olafsen and J. S. Urbach. Clustering, order, and collapse in a driven granular monolayer. Physical Review Letters, 81:4369–4372, Nov 1998.

[68] René Zuñiga, Germán Varas, and Stéphane Job. Geometry-controlled phase transition in vibrated granular media. Scientific Reports, 12(1):14989, 2022.

[69] Francisco Vega Reyes and Jeffrey S Urbach. Effect of inelasticity on the phase transitions of a thin vibrated granular layer. Physical Review E—Statistical, Nonlinear, and Soft Matter Physics, 78(5):051301, 2008.

[70] Alexander E Lobkovsky, F Vega Reyes, and JS Urbach. The effects of forcing and dissipation on phase transitions in thin granular layers. The European Physical Journal Special Topics, 179(1):113–122, 2009.

[71] Guoxian Gao, Yanpei Chen, Ji Xu, Kai Li, and Bona Lu. Temperature inversion across coexisting phases in two-dimensional driven granular materials. Physics of Fluids, 36(12), 2024.

[72] A Plati, R Maire, F Boulogne, F Restagno, F Smallenburg, and G Foffi. Self-assembly and non-equilibrium phase coexistence in a binary granular mixture. arXiv preprint arXiv:2410.21576, 2024.

[73] R Maire, A Plati, M Stockinger, E Trizac, F Smallenburg, and G Foffi. Interplay between an absorbing phase transition and synchronization in a driven granular system. Physical Review Letters, 132(23):238202, 2024.

[74] Andrea Plati, Raphael Maire, Etienne Fayen, Fran-

cois Boulogne, Frederic Restagno, Frank Smallenburg, and Giuseppe Foffi. Quasi-crystalline order in vibrating granular matter. Nature Physics, 20(3):465–471, 2024.
[75] Gustavo Castillo, Nicolás Mujica, and Rodrigo Soto. Fluctuations and criticality of a granular solid-liquid-like phase transition. Physical Review Letters, 109(9):095701, 2012.
[76] Gustavo Castillo, Nicolás Mujica, and Rodrigo Soto. Universality and criticality of a second-order granular solid-liquid-like phase transition. Physical Review E, 91(1):012141, 2015.
[77] Marcelo Guzmán and Rodrigo Soto. Critical phenomena in quasi-two-dimensional vibrated granular systems. Physical Review E, 97(1):012907, 2018.
[78] W. Losert, D. G. W. Cooper, and J. P. Gollub. Propagating front in an excited granular layer. Physical Review E, 59:5855–5861, May 1999.
[79] Alexis Prevost, Paul Melby, David A. Egolf, and Jeffrey S. Urbach. Nonequilibrium two-phase coexistence in a confined granular layer. Physical Review E, 70:050301, Nov 2004.
[80] M. Argentina, M. G. Clerc, and R. Soto. van der waals–like transition in fluidized granular matter. Physical Review Letters, 89:044301, Jul 2002.
[81] Gustavo Castillo, Nicolás Mujica, Néstor Sepúlveda, Juan Carlos Sobarzo, Marcelo Guzmán, and Rodrigo Soto. Hyperuniform states generated by a critical friction field. Physical Review E, 100(3):032902, 2019.
[82] Pedro M Reis, Rohit A Ingale, and Mark D Shattuck. Crystallization of a quasi-two-dimensional granular fluid. Physical review letters, 96(25):258001, 2006.
[83] Ricardo Brito, Dino Risso, and Rodrigo Soto. Hydrodynamic modes in a confined granular fluid. Physical Review E—Statistical, Nonlinear, and Soft Matter Physics, 87(2):022209, 2013.
[84] A Sarracino, D Villamaina, G Costantini, and A Puglisi. Granular brownian motion. Journal of Statistical Mechanics: Theory and Experiment, 2010(04):P04013, apr 2010.
[85] Andrea Puglisi. Transport and fluctuations in granular fluids: From Boltzmann equation to hydrodynamics, diffusion and motor effects. Springer, 2014.
[86] R. Maire and A. Plati. Enhancing (quasi-)long-range order in a two-dimensional driven crystal. The Journal of Chemical Physics, 161(5):054902, 08 2024.
[87] Etienne P Bernard and Werner Krauth. Two-step melting in two dimensions: first-order liquid-hexatic transition. Physical review letters, 107(15):155704, 2011.
[88] Linge Bai and David Breen. Calculating center of mass in an unbounded 2d environment. Journal of Graphics Tools, 13(4):53–60, 2008.
[89] Claudio Maggi, Matteo Paoluzzi, Andrea Crisanti, Emanuela Zaccarelli, and Nicoletta Gnan. Universality class of the motility-induced critical point in large scale off-lattice simulations of active particles. Soft Matter, 17(14):3807–3812, 2021.
[90] Jonathan Tammo Siebert, Florian Dittrich, Friederike Schmid, Kurt Binder, Thomas Speck, and Peter Virnau. Critical behavior of active brownian particles. Physical Review E, 98(3):030601, 2018.
[91] Frank Smallenburg. Efficient event-driven simulations of hard spheres. The European Physical Journal E, 45(3):22, 2022.
[92] Andrea Baldassarri, Alain Barrat, G D'anna, Vittorio Loreto, P Mayor, and A Puglisi. What is the temperature of a granular medium? Journal of physics: condensed matter, 17(24):S2405, 2005.
[93] A Puglisi, A Sarracino, and A Vulpiani. Temperature in and out of equilibrium: A review of concepts, tools and attempts. Physics Reports, 709:1–60, 2017.
[94] Joseph E Mayer and Wm W Wood. Interfacial tension effects in finite, periodic, two-dimensional systems. The Journal of Chemical Physics, 42(12):4268–4274, 1965.
[95] Michael Engel, Joshua A Anderson, Sharon C Glotzer, Masaharu Isobe, Etienne P Bernard, and Werner Krauth. Hard-disk equation of state: First-order liquid-hexatic transition in two dimensions with three simulation methods. Physical Review E—Statistical, Nonlinear, and Soft Matter Physics, 87(4):042134, 2013.
[96] Botao Li, Yoshihiko Nishikawa, Philipp Höllmer, Louis Carillo, AC Maggs, and Werner Krauth. Hard-disk pressure computations—a historic perspective. The Journal of Chemical Physics, 157(23), 2022.
[97] I Pagonabarraga, E Trizac, TPC Van Noije, and MH Ernst. Randomly driven granular fluids: Collisional statistics and short scale structure. Physical Review E, 65(1):011303, 2001.
[98] Vicente Garzó, Ricardo Brito, and Rodrigo Soto. Enskog kinetic theory for a model of a confined quasi-two-dimensional granular fluid. Physical Review E, 98(5):052904, 2018.
[99] Baptiste Néel, Ignacio Rondini, Alex Turzillo, Nicolás Mujica, and Rodrigo Soto. Dynamics of a first-order transition to an absorbing state. Physical Review E, 89(4):042206, 2014.
[100] Jean-Pierre Hansen and Ian Ranald McDonald. Theory of simple liquids: with applications to soft matter. Academic press, 2013.
[101] Giacomo Gradenigo, Alessandro Sarracino, Dario Villamaina, and Andrea Puglisi. Fluctuating hydrodynamics and correlation lengths in a driven granular fluid. Journal of Statistical Mechanics: Theory and Experiment, 2011(08):P08017, 2011.
[102] Alain Barrat and Emmanuel Trizac. Molecular dynamics simulations of vibrated granular gases. Physical Review E, 66(5):051303, 2002.
[103] TPC Van Noije, MH Ernst, Emmanuel Trizac, and I Pagonabarraga. Randomly driven granular fluids: Large-scale structure. Physical Review E, 59(4):4326, 1999.
[104] Marjolein de Jager, Carlos Vega, Pablo Montero de Hijes, Frank Smallenburg, and Laura Filion. Statistical mechanics of crystal nuclei of hard spheres. arXiv preprint arXiv:2407.04394, 2024.
[105] Nikolai V Brilliantov and Thorsten Pöschel. Kinetic theory of granular gases. Oxford University Press, USA, 2004.
[106] TPC Van Noije and MH Ernst. Velocity distributions in homogeneous granular fluids: the free and the heated case. Granular Matter, 1(2):57–64, 1998.
[107] Sergei E Esipov and Thorsten Pöschel. The granular phase diagram. Journal of statistical physics, 86:1385–1395, 1997.
[108] GW Baxter and JS Olafsen. Experimental evidence for molecular chaos in granular gases. Physical review letters, 99(2):028001, 2007.
[109] Rubén Gómez González, Vicente Garzó, Ricardo Brito, and Rodrigo Soto. Diffusion of impurities in a moder-

ately dense confined granular gas. Physics of Fluids, 36(12), 2024.

[110] Nikolai V Brilliantov and Thorsten Pöschel. Breakdown of the sonine expansion for the velocity distribution of granular gases. Europhysics Letters, 74(3):424, 2006.

[111] J-C Géminard and C Laroche. Energy of a single bead bouncing on a vibrating plate: Experiments and numerical simulations. Physical Review E, 68(3):031305, 2003.

[112] Etienne Fayen, Anuradha Jagannathan, Giuseppe Foffi, and Frank Smallenburg. Infinite-pressure phase diagram of binary mixtures of (non) additive hard disks. The Journal of chemical physics, 152(20), 2020.

[113] Etienne Fayen, Marianne Impéror-Clerc, Laura Filion, Giuseppe Foffi, and Frank Smallenburg. Self-assembly of dodecagonal and octagonal quasicrystals in hard spheres on a plane. Soft Matter, 19(14):2654–2663, 2023.

[114] Etienne Fayen, Laura Filion, Giuseppe Foffi, and Frank Smallenburg. Quasicrystal of binary hard spheres on a plane stabilized by configurational entropy. Physical Review Letters, 132(4):048202, 2024.

[115] Gustavo M Rodríguez-Liñán and Marco Heinen. Granular beads in a vibrating, quasi two-dimensional cell: The true shape of the effective pair potential. Journal of Computational Physics, 394:232–242, 2019.

[116] RA Bordallo-Favela, A Ramírez-Saíto, CA Pacheco-Molina, JA Perera-Burgos, Y Nahmad-Molinari, and G Pérez. Effective potentials of dissipative hard spheres in granular matter. The European Physical Journal E, 28:395–400, 2009.

[117] Stephanie Velázquez-Pérez, Gabriel Pérez-Ángel, and Yuri Nahmad-Molinari. Effective potentials in a bidimensional vibrated granular gas. Physical Review E, 94(3):032903, 2016.

[118] John Michael Kosterlitz and David James Thouless. Ordering, metastability and phase transitions in two-dimensional systems. In Basic Notions Of Condensed Matter Physics, pages 493–515. CRC Press, 2018.

[119] BI Halperin and David R Nelson. Theory of two-dimensional melting. Physical Review Letters, 41(2):121, 1978.

[120] David R Nelson and BI Halperin. Dislocation-mediated melting in two dimensions. Physical Review B, 19(5):2457, 1979.

[121] AP Young. Melting and the vector coulomb gas in two dimensions. Physical Review B, 19(4):1855, 1979.

[122] VL314399 Berezinskii. Destruction of long-range order in one-dimensional and two-dimensional systems having a continuous symmetry group i. classical systems. Sov. Phys. JETP, 32(3):493–500, 1971.

[123] Óscar Toledano, M Pancorbo, JE Alvarellos, and Óscar Gálvez. Melting in two-dimensional systems: Characterizing continuous and first-order transitions. Physical Review B, 103(9):094107, 2021.

[124] Sebastian C Kapfer and Werner Krauth. Two-dimensional melting: From liquid-hexatic coexistence to continuous transitions. Physical review letters, 114(3):035702, 2015.

[125] Leonardo Galliano, Michael E Cates, and Ludovic Berthier. Two-dimensional crystals far from equilibrium. Physical Review Letters, 131(4):047101, 2023.

[126] Yuta Kuroda, Takeshi Kawasaki, and Kunimasa Miyazaki. Long-range translational order and hyperuniformity in two-dimensional chiral active crystal. arXiv preprint arXiv:2402.19192, 2024.

[127] Yann-Edwin Keta and Silke Henkes. Long-range order in two-dimensional systems with fluctuating active stresses, 2024.

[128] Rodrigo Soto and Michel Mareschal. Statistical mechanics of fluidized granular media: Short-range velocity correlations. Physical Review E, 63(4):041303, 2001.

[129] Paolo Visco, Frédéric van Wijland, and Emmanuel Trizac. Collisional statistics of the hard-sphere gas. Physical Review E—Statistical, Nonlinear, and Soft Matter Physics, 77(4):041117, 2008.